

Facile preparation of EDTA-functionalized chitosan magnetic adsorbent for removal of Pb(II)

Zhengyan Tan,¹ Hong Peng,¹ Hongfang Liu,¹ Linling Wang,² Jing Chen,² Xiaohua Lu¹

¹Institute of Inorganic Chemistry and Chemical Biology, School of Chemistry and Chemical Engineering, Huazhong University of Science and Technology, Wuhan 430074, People's Republic of China

²Environmental Science Research Institute, School of Environmental Science and Engineering, Huazhong University of Science and Technology, Wuhan 430074, People's Republic of China

Correspondence to: H. Peng (E-mail: penghong811@163.com)

ABSTRACT: A novel magnetic adsorbent (EDTA/chitosan/PMMS) was facilely prepared by reacting chitosan with EDTA anhydride in presence of PEI-coated magnetic microspheres. The as-synthesized EDTA/chitosan/PMMS was characterized by XRD, SEM, TGA, FT-IR, and VSM, and then employed in removal of heavy metals of Pb(II) from aqueous solution. The results of the batch adsorption experiments revealed that the adsorbents had extremely high uptake capacities for Pb(II) in the pH range of 2 to 5.5, and the adsorption kinetics for EDTA/chitosan/PMMS was consistent with the pseudo-second-order kinetic model. Moreover, its equilibrium data were fitted with the Langmuir isothermal model well, which indicated that the adsorption mechanism was a homogeneous monolayer chemisorptions process. The maximum adsorption capacity of EDTA/chitosan/PMMS for Pb(II) was found to be 210 mg g⁻¹ at pH 4 (30°C), and further reuse experiments results suggested that EDTA/chitosan/PMMS could be a potential recyclable magnetic adsorbent in the practical wastewater treatment. © 2015 Wiley Periodicals, Inc. *J. Appl. Polym. Sci.* **2015**, *132*, 42384.

KEYWORDS: adsorption; biopolymers & renewable polymers; crosslinking; magnetism and magnetic properties

Received 7 August 2014; accepted 19 April 2015

DOI: 10.1002/app.42384

INTRODUCTION

In recent years, water pollution by heavy metals has triggered a grievous threat to ecological system as well as public health due to their highly toxic and mutagenic properties. Within such heavy metals, lead (Pb (II)) has been considered as one of most harmful ions owing to its serious neurotoxicity, blood and reproductive toxicity. Traditional technologies developed for removal of lead from aqueous stream are chemical precipitation,¹ ion exchange,² membrane filtration,³ electrolytic means,⁴ reverse osmosis,⁵ and adsorption.⁶ In the past few decades, biosorption methods using biomass,⁷ natural polymers,^{8–10} or agricultural wastes¹¹ as adsorbents for removal of heavy metals have been gained increasing attention on account of its good performance, low cost, and eco-friendly application process.

Chitosan, deacetylation product of chitin, which is the second most abundant biopolymer present in nature, has been proved to be an excellent and cheap adsorbent for heavy metals because of its large amounts of amino and hydroxyl functional groups.¹² In order to further improve its removal efficiency for heavy metals, modification of chitosan with more effective chelating groups such as dibenzocrown ether,¹³ tripolyphosphate,¹⁴ dithiocarba-

mate,¹⁵ DTPA,¹⁶ and EDTA¹⁶ is one of promising methods. However, EDTA-functionalized chitosan adsorbents are not easily separated from aqueous media due to its notable swelling properties.¹⁷ Magnetic separation techniques might solve this problem conveniently by incorporating magnetic cores into EDTA-modified chitosan. Recently, one kind of chitosan-EDTA enwrapped magnetic CoFe₂O₄ nanoparticles prepared via emulsion cross-linking method was reported by employing the water-soluble 1-ethyl-3-(3-dimethylaminopropyl) carbodiimide hydrochloride (EDAC) as the cross-linker,¹⁸ and a novel magnetic EDTA-modified chitosan/SiO₂/Fe₃O₄ adsorbent (EDCMS) was also developed by surface modification of chitosan/SiO₂/Fe₃O₄ (CMS) with EDTA using EDAC as the cross-linker in buffer solution.¹⁹

In this article, a facile approach for preparation of EDTA-functionalized chitosan magnetic adsorbent was reported, where polyethylene imine (PEI) coated magnetic microspheres were used as magnetic cores, and EDTA anhydride was employed as the cross-linker of chitosan and magnetic cores in an aqueous solution of methanol and acetic acid. In this method, not only was chitosan cross-linked and functionalized by EDTA ligands, but also magnetic microspheres could be embedded in chitosan

at the same time. Moreover, the amino groups of PEI on magnetic microspheres could react with EDTA anhydride, which could result in the crosslink of magnetic cores with chitosan through chemical bonds, and inhibit it from leaking out of crosslinked chitosan in the application processes. In this article, the synthesized magnetic adsorbents were further characterized, and their adsorption properties for removal of Pb(II) from aqueous solution under various experimental conditions were also investigated.

EXPERIMENTAL

Materials and Techniques

Ferric chloride hexahydrate and ethylene glycol were purchased from Sinopharm Chemical Reagent Co., Ltd. (Shanghai, China). Polyethyleneimine (PEI 600) ($M_w = 600$ g/mol) and polyethyleneimine (PEI 10,000) ($M_w = 10,000$ g/mol) of 99% purity were bought from Aladdin Industrial Corporation (Shanghai, China). EDTA anhydride were purchased from Tokyo Chemical Industry Co., Ltd., and Chitosan (90% degree of deacetylation) was bought from Ruji Biology Technology Co., Ltd. (Shanghai, China). All chemicals were of analytical grade or commercially available, and were used without further purification.

X-ray diffraction analysis (XRD) was recorded on an X'Pert PRO X-ray diffractometer (PANalytical B.V., Netherlands) at room temperature. The morphology and the sizes of products were characterized by a Sirion 200 field emission scanning electron microscopy (FE-SEM, FEI Co., Netherlands). Infrared spectra were carried out by using an Equinox 55 Fourier transform infrared spectrometer (FT-IR, Bruker Optics, Germany). Thermogravimetric analysis (TGA) was performed with a Diamond TG/DTA (PerkinElmer Instruments, China) and tests were conducted under a dynamic nitrogen atmosphere flowing, and the heating rate is $15^\circ\text{C min}^{-1}$. The magnetic properties of samples were measured at room temperature with a Lake Shore 7410 vibrating sample magnetometer (VSM, Lake Shore). An Agilent 4100 Microwave Plasma-Atomic Emission Spectrometer (MP-AES, Agilent Technologies, Australia) was employed to determine the concentrations of Pb(II) ions.

Preparation of Magnetic Microspheres

The magnetic microspheres (MMS) were prepared by a modified solvothermal reduction process according to the previous work.²⁰ $\text{FeCl}_3 \cdot 6\text{H}_2\text{O}$ (5.0 g) was dissolved into ethylene glycol (150 mL) to form orange transparent solution. Then NaAc (13.5 g), PEG 200 (3.75 g), and PEI 600 (1.8 g) were added into the solution to form emulsion mixture under vigorous stirring for 30 min. Finally the emulsion was sealed into Teflon-lined stainless-steel autoclaves, and kept at 200°C for 8 h. The black products were successively washed with ethanol and deionized water for several times, and dried at 50°C in a vacuum oven for 12 h.

Preparation of PEI 10,000 Coated Magnetic Microspheres

The PEI 10,000 coated magnetic microspheres (PMMS) were synthesized by a modified procedure as referred in the literature.²¹ 1.8 g of PEI 10,000 was firstly dissolved into 40 mL of DMF organic solvent, and then as-synthesized MMS (0.2 g) were dispersed into the organic solution under ultrasonication

vibration for 30 min, followed by continuously stirring for 24 h. After magnetic separation, PMMS was washed with ethanol for several times, and dried at 50°C in a vacuum oven for 12 h.

Preparation of EDTA-Functionalized Chitosan Magnetic Adsorbent

The preparation procedure for EDTA-modified chitosan was described in previous report.¹⁶ Based on this report, EDTA-functionalized chitosan magnetic adsorbent (EDTA/chitosan/PMMS) were prepared by following steps: 0.175 g of chitosan was dissolved into 5 mL of HAc aqueous solution (10% v/v), and then diluted with 30 mL of methanol. Then, 100 mg of PMMS particles were dispersed into the chitosan-methanol solution, followed by stage addition of EDTA anhydride (total 1.5 g) under ultrasonication vibration. After that, the mixture was kept under ultrasonication vibration for another 30 min, and then continuously stirred for 24 h. When the reaction was over, the products (EDTA/chitosan/PMMS) were removed from methanol solution by magnetic separation, and then dispersed into 40 mL of ethanol by vigorously stirring for 24 h. Afterwards, EDTA/chitosan/PMMS was washed with water and then with Na_2HPO_4 solution to remove unreacted EDTA. Finally, washed with deionized water, 0.1M HCl, and again deionized water. The products were dried at 50°C in a vacuum oven for 48 h, then ground to sieve by a 300 meshes sieve, and stored in the desiccator.

Adsorption and Desorption Experiments

Batch adsorption experiments were generally operated by agitating the flasks containing EDTA/chitosan/PMMS and solutions of Pb(II) ion on a rotary shaker.

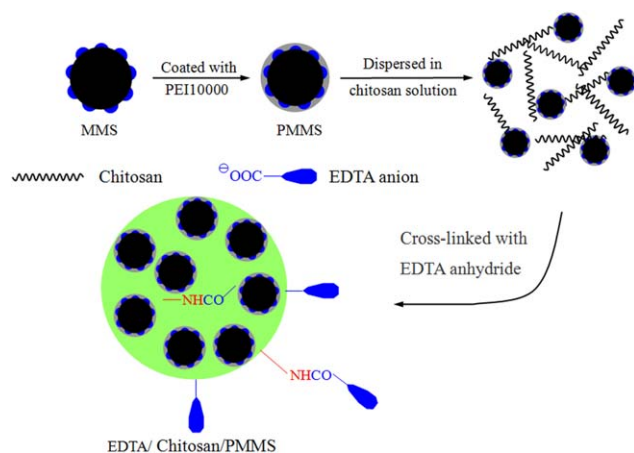
For the influence of pH on the adsorption, the experiment was carried out at the following conditions: the initial concentration of Pb(II) ions is 150 mg L^{-1} in the pH range of 1 to 5.5 at 25°C , and the dosage of the adsorbent is 0.67 g L^{-1} . The pH values of the solutions were adjusted using 0.01M nitric acid or/and sodium hydroxide aqueous solutions.

To explore the isotherms, the batch adsorption was conducted at the initial concentrations of Pb(II) ions varying from 160 to 420 mg L^{-1} . For the kinetic study, 50.0 mg of adsorbents were dispersed in 50.0 mL of Pb(II) ion solution (210 mg L^{-1}) at pH 4, and kept continuously stirring for 24 h. At designed time intervals, 1 mL of the suspension was taken out to determine the concentration of Pb(II) ions by MP-AES. The adsorption capacities for Pb(II) ions (q_e , mmol g^{-1}) were calculated as follows:

$$q_e = \frac{C_0 - C_e}{m} V \quad (1)$$

where C_0 and C_e (mM) are the initial and the equilibrium concentrations of Pb(II) ions, respectively. V (L) is the volume of the solution whereas m (g) represents the weight of the adsorbent.

To explore the reusability of EDTA/chitosan/PMMS, 10 mg of dry adsorbents were loaded with Pb(II) ions using 10.0 mL of 240 mg L^{-1} metal ion solution at 30°C and pH 4.0 for 24 h on a rotary shaker. The Pb(II)-loaded adsorbent was collected, and washed with water to remove the un-adsorbed Pb(II) ions. The



Scheme 1. The procedures for preparation of magnetic adsorbents of EDTA/chitosan/PMMS. [Color figure can be viewed in the online issue, which is available at wileyonlinelibrary.com.]

adsorbent was then agitated with 10.0 mL of 0.1M Na₂EDTA for another 12 h. After desorption of Pb(II) ions, the adsorbents were washed with 0.1M disodium hydrogen phosphate, then with water for several times for the next step of reuse. This adsorption–desorption cycle was repeated five times by using the same adsorbent.

RESULTS AND DISCUSSION

Preparation and Characterization of EDTA/Chitosan/PMMS

The procedure for preparation of EDTA/chitosan/PMMS magnetic adsorbents is presented in Scheme 1, and the cross-linking reaction mechanism of EDTA anhydride taking place in the preparation procedure is shown in Scheme 2. It can be seen that EDTA anhydride has several important roles in the preparation process. Firstly, EDTA anhydride could act as cross-linker to react with the amino groups of chitosan, and then result in forming chitosan gels through amide bonds; Secondly, EDTA anhydride could act as reaction agents to modify the residue amino groups of chitosan with EDTA chelating groups; Thirdly, EDTA anhydride could act as coupling agents to induce the linkage of PMMS and chitosan gels via amide bonds, which could inhibit PMMS from leaking out of chitosan gels in the application procedure.

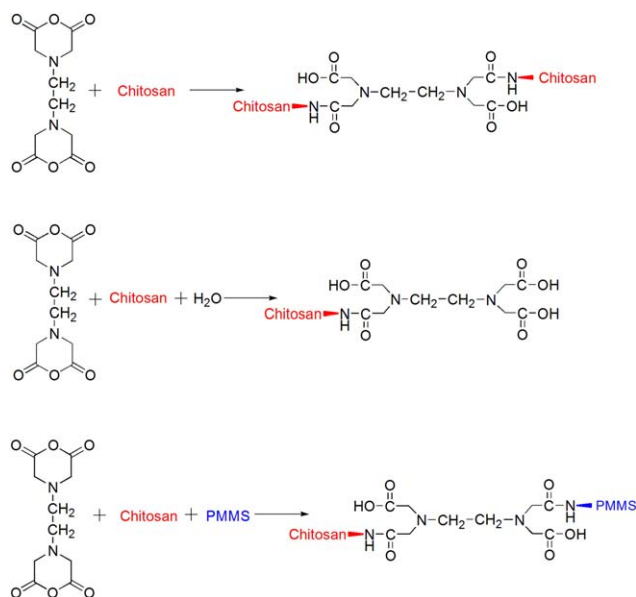
The successful preparation of EDTA/chitosan/PMMS magnetic adsorbents could be intuitively observed from the images of field emission scanning electron microscope (FE-SEM) shown in Figure 1. It can be seen from Figure 1(a) that PEI 600 modified magnetic microspheres (MMS) are in good spherical shape with diameters mainly ranging from 200 to 500 nm. In order to improve the amounts of amino groups on the surfaces of MMS, PEI 10,000 was further coated on MMS, and the morphology of this material (PMMS) is displayed in Figure 1(b). It is obviously seen that the surfaces of magnetic microspheres look like more smooth than that of MMS, and some magnetic microspheres are clung together by slight amount of polymer, suggesting that PEI 10,000 was deposited on MMS. As presented in Figure 1(c), the FE-SEM image of EDTA/chitosan/PMMS illustrates that some PMMS microspheres are embedded inside the cross-linked

chitosan, while some are mounted on the surface of the cross-linked chitosan. However, naked PMMS has not been found, indicating that crosslink of PMMS and chitosan by EDTA anhydride is very successful due to PEI 10,000 coated on magnetic microspheres.

The XRD patterns of the samples, including MMS, PMMS, and EDTA/chitosan/PMMS, are depicted in Figure 2. The characteristic diffraction peaks appeared in MMS at 30.1°, 35.4°, 43.1°, 53.4°, 56.9°, and 62.5° could be assigned to be [220], [311], [400], [422], [511], and [440] planes of magnetite (JCPDS card No.19–0629), respectively. The XRD patterns of PMMS and EDTA/chitosan/PMMS are both in agreement with that of MMS, indicating that the whole synthesis processes did not result in the significant phase change of magnetic cores.

The weight proportion of organic polymers grafted on PMMS could be estimated from TGA analysis, which is given in Figure 3. The TGA curve of MMS shows the weight loss over temperature ranging from 200°C to 900°C is about 2.9% (Figure 3, curve a), which might be related to the escape of PEI 600 modified on MMS. For PMMS, the weight loss from 200°C to 900°C is about 5.2% (Figure 3, curve b), which is attributed to the degradation of PEI 10,000 and PEI 600 coated on magnetic microspheres. As organic polymers were usually decomposed completely over the temperature ranging from 200°C to 700°C, the weight percentage of EDTA modified chitosan on EDTA/chitosan/PMMS could be estimated to be 64.4%, based on the weight loss from curve c.

The evidence of existence of EDTA/chitosan/PMMS could be further achieved by FT-IR analysis. For MMS magnetic cores, the strong absorption peak at 577 cm⁻¹ is observed in Figure 4 (curve a), which is attributed to the stretching vibration of Fe–O bond of magnetite. However, apart from this typical peak, the characterized absorption peaks for PEI 600 on MMS



Scheme 2. Cross-linking reaction mechanisms of EDTA anhydride in the process of preparation of EDTA/chitosan/PMMS. [Color figure can be viewed in the online issue, which is available at wileyonlinelibrary.com.]

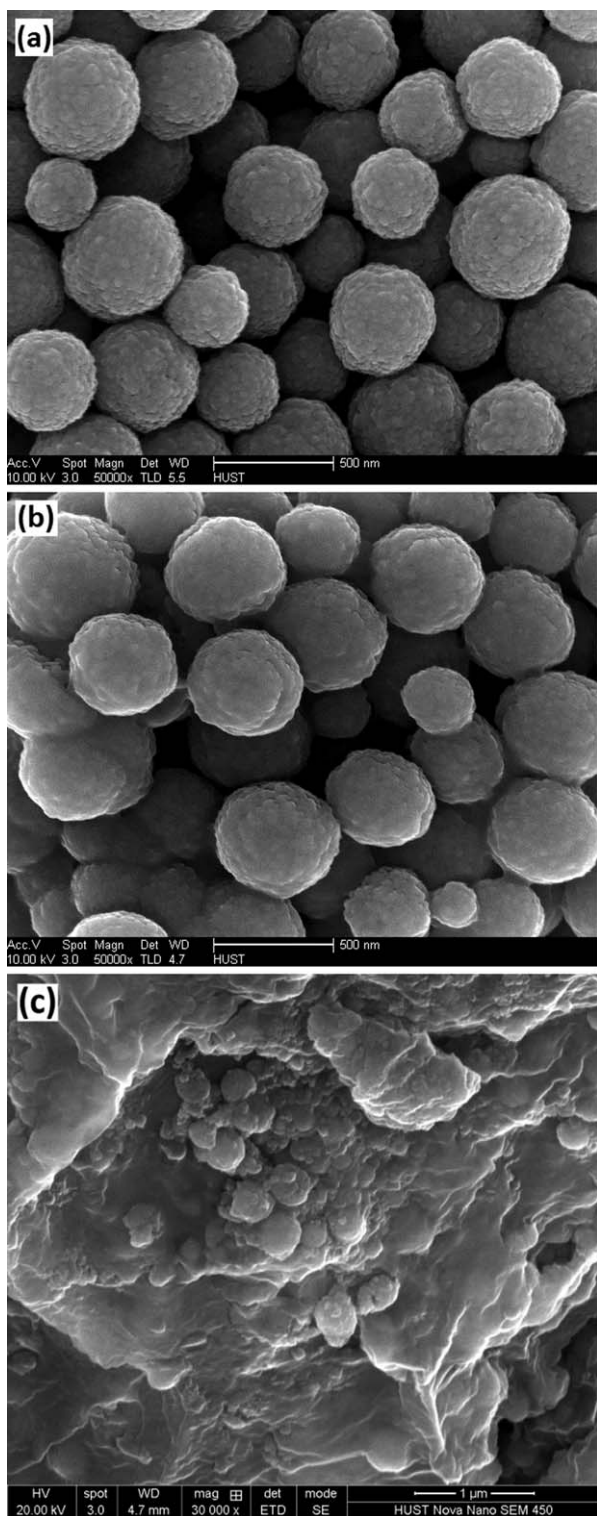


Figure 1. FE-SEM micrographs of (a) MMS, (b) PMMS and (c) EDTA/chitosan/PMMS.

can not be seen obviously due to very low PEI grafted ratio (about 2.9%). Although the strength of a pair of absorption peaks appeared at 2922 and 2853 cm^{-1} (symmetric and anti-symmetric C—H stretch of CH_2) increase slightly (shown in curve b), the peak attributions for PEI on PMMS can not be

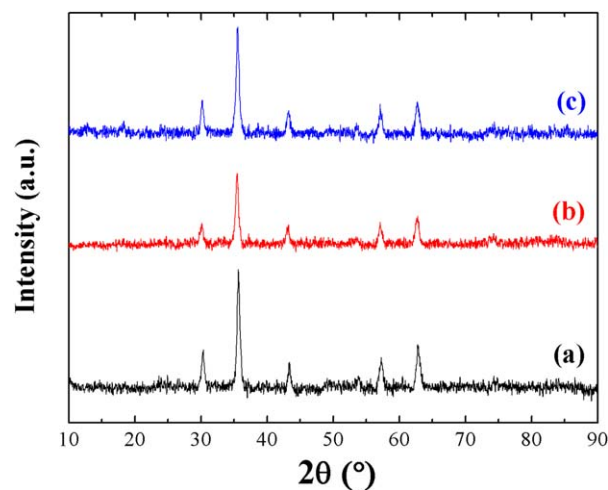


Figure 2. XRD patterns of (a) MMS, (b) PMMS, and (c) EDTA/chitosan/PMMS. [Color figure can be viewed in the online issue, which is available at wileyonlinelibrary.com.]

observed very clearly either, because PEI-coated on MMS is about 5.2% based on TGA results. Nevertheless, as given in Figure 4 (curve c), the major characterized absorption peaks for EDTA/chitosan/PMMS could be observed obviously and assigned as follows: 1738 cm^{-1} (the carbonyl stretch of COOH groups from EDTA modified adsorbents); 1633 cm^{-1} (C=O stretching vibrations of amide groups generated from the cross-linking of chitosan with EDTA anhydride);²² 1396 cm^{-1} (C—O stretching vibration of the $-\text{COO}^-$ groups from EDTA modified chitosan);¹⁸ 1067 cm^{-1} (C—O—C stretching vibration in chitosan ring backbone);²³ 1031 cm^{-1} (skeletal vibration of C—O stretching). Moreover, compared with curve a and curve b, the area for the stretching vibrations of Fe—O bond in EDTA/chitosan/PMMS becomes more broad, suggesting the further oxidation of PMMS during the cross-linking reaction in HAc solution.

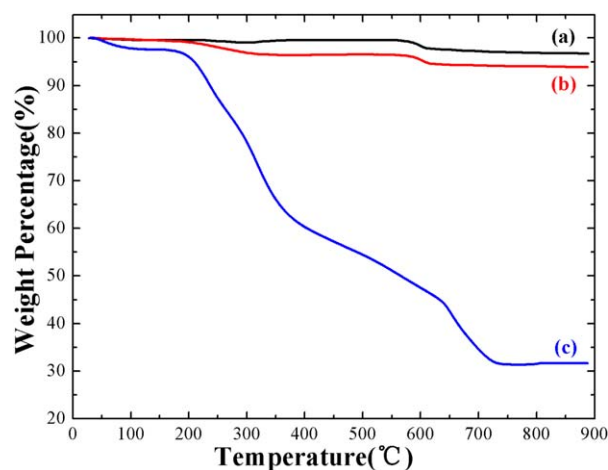


Figure 3. TGA curves of (a) MMS, (b) PMMS and (c) EDTA/chitosan/PMMS. [Color figure can be viewed in the online issue, which is available at wileyonlinelibrary.com.]

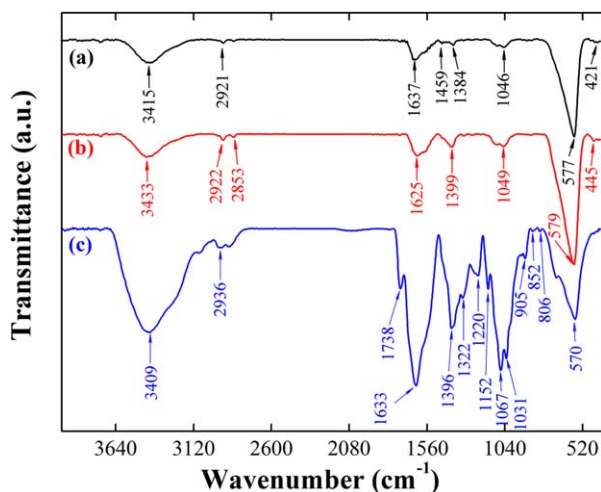


Figure 4. FT-IR spectra of (a) MMS, (b) PMMS and (c) EDTA/chitosan/PMMS. [Color figure can be viewed in the online issue, which is available at wileyonlinelibrary.com.]

The magnetic hysteresis loops of samples are shown in Figure 5. The saturation magnetizations are found to be 78.9, 73.5, and 20.1 emu g^{-1} for MMS, PMMS, and EDTA/chitosan/PMMS, respectively. The decreases in saturation magnetizations might be mainly responsible for the deposition of PEI 10,000 and coating of EDTA modified chitosan on the surfaces of the magnetic microspheres. Additionally, the surfaces of PMMS might be partially oxidated in the preparation process of EDTA/chitosan/PMMS under acid conditions, which might result in the decrease of saturation magnetization. Furthermore, physical water and structure water adsorbed on EDTA/chitosan/PMMS might also reduce the saturation magnetization.¹⁹ However, from the upper and the nether insets of Figure 5, it can be seen that EDTA/chitosan/PMMS are attracted strongly toward the permanent magnet within several seconds, demonstrating directly that they possess excellent magnetic separability in aqueous solution.

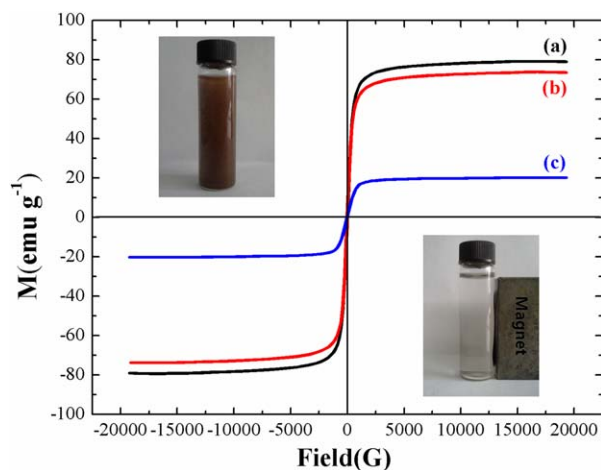


Figure 5. Magnetic hysteresis loops of (a) MMS, (b) PMMS, and (c) EDTA/chitosan/PMMS (insets: magnetic separation of EDTA/chitosan/PMMS from aqueous suspensions). [Color figure can be viewed in the online issue, which is available at wileyonlinelibrary.com.]

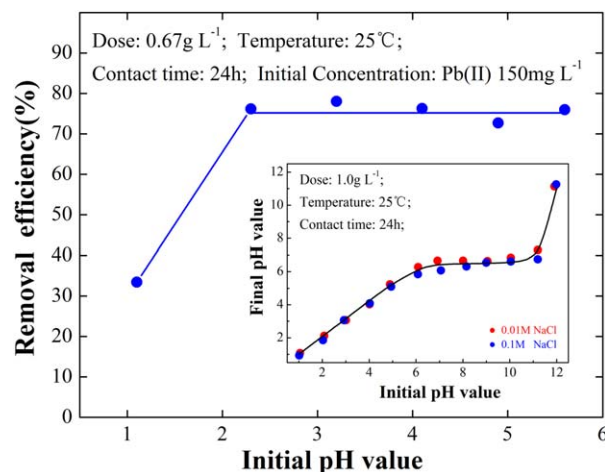


Figure 6. Effect of pH on the adsorption of Pb(II) ions by EDTA/chitosan/PMMS (inset: determination of pHzpc of EDTA/chitosan/PMMS in NaCl solutions). [Color figure can be viewed in the online issue, which is available at wileyonlinelibrary.com.]

Effect of pH on Adsorption of Pb(II)

The pH of the aqueous solution is an important operational parameter in the adsorption process, since pH values affect not only protonation of the functional groups of the adsorbent, but also the speciation of heavy metal ions in solution.¹⁶ Effect of initial pH value on Pb(II) ions adsorbed by EDTA/chitosan/PMMS is described in Figure 6. The removal efficiency of the adsorbent for Pb(II) increases sharply with the pH value increasing from 1 to 2, then reaches a plateau at pH beyond 2.0, which presents a similar trend as that obtained from EDTA-modified chitosan-silica hybrid materials.¹⁷

The pHzpc of EDTA/chitosan/PMMS was determined by simple batch equilibrium method²⁴ using NaCl (0.1 and 0.01M) as background electrolyte, and found to be 6.5 ± 0.2 , which is shown in the inset of Figure 6. In generally speaking, the adsorption capacities for cationic metal ions (Pb^{2+} or $[\text{Pb}(\text{OH})]^+$) on the adsorbent would increase gradually until solution $\text{pH} > \text{pHzpc}$.²⁵ For example, the higher adsorption capacity for Pb^{2+} on CMS¹⁹ (an unmodified magnetic chitosan adsorbent) was achieved at solution pH value > 4 , and its adsorption capacity was nearly zero when solution $\text{pH} < 3$. However, as presented in Figure 6, the uptake capacity of Pb^{2+} on EDTA/chitosan/PMMS reaches a plateau at pH beyond 2.0 ($< \text{pHzpc}$), which is attributed to the excellent chelating properties of EDTA groups for Pb(II) at low pH values. The main species of lead-EDTA complexes could be hypothesized as complex A and complex B, which are shown in Figure 7. There are four chelating rings in complex A and three chelating rings in complex B, which is the reason why lead-EDTA complexes were so stable at very low pH values. Besides, in the complex A or B, the positions of water could be also replaced by hydroxyl groups or amino groups of chitosan on the adsorbent of EDTA/chitosan/PMMS, which might improve the stability of the lead-EDTA complexes further.

As the erosion of the magnetic cores embedded in the adsorbents under strong acid conditions should be considered, and the

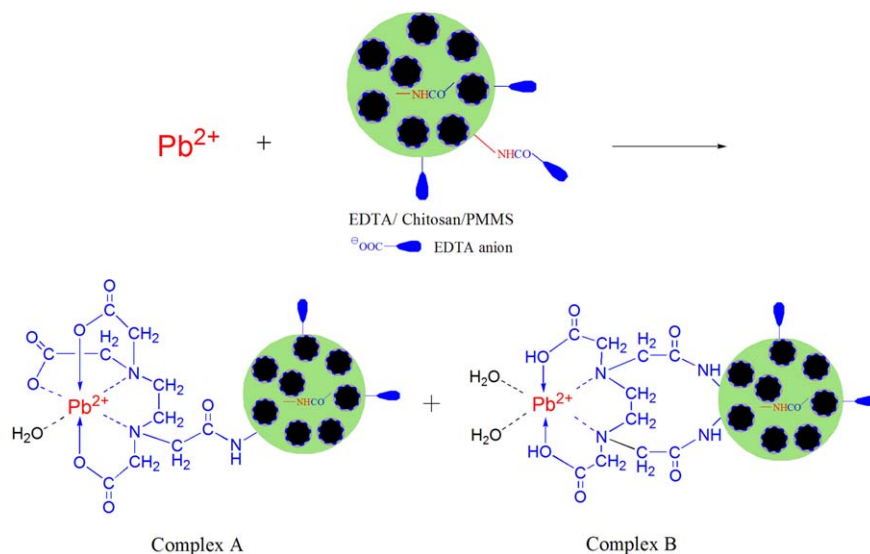


Figure 7. The main species of lead-EDTA complexes formed in aqueous solution of Pb(II) ions with EDTA/chitosan/PMMS. [Color figure can be viewed in the online issue, which is available at wileyonlinelibrary.com.]

probability of the formation of metal hydroxide precipitates for Pb(II) might be happened at pH above 5.5, pH 4.0 was selected as the optimum pH value in the following experiments.

Effect of Contact Time on Adsorption and Kinetic Studies

The effect of contact time on the adsorption of Pb(II) by EDTA/chitosan/PMMS is shown in Figure 8. It can be seen that adsorption was rapid initially, and slowed down thereafter, finally reached equilibrium. In order to investigate the rate-controlling step in the adsorption mechanisms, the kinetic experimental data presented in Figure 8(a) were dealt with Lagergren's pseudo-first-order,²⁶ Ho's pseudo-second-order,²⁷ intraparticle diffusion kinetic models,²⁸ respectively, and the linear form equations of the three models can be written as follows:

The pseudo-first-order model:

$$\ln(q_e - q_t) = \ln q_e - k_1 t \quad (2)$$

The pseudo-second-order model:

$$\frac{t}{q_t} = \frac{1}{k_2 q_e^2} + \frac{1}{q_e} t \quad (3)$$

The intraparticle diffusion kinetic model:

$$q_t = k_{id} t^{1/2} + c \quad (4)$$

where q_t and q_e (mg g^{-1}) are the uptake capacity of Pb(II) onto the adsorbent at any time t and at equilibrium, respectively. The parameters of k_1 (min^{-1}) and k_2 ($\text{g mg}^{-1} \text{min}^{-1}$) are the rate constants of the pseudo-first-order and pseudo-second-order models, respectively. k_{id} ($\text{mg g}^{-1} \text{min}^{-1/2}$) is the intraparticle diffusion rate constant. C is the thickness of the boundary layer.

The kinetic parameters obtained from simulating the experimental data with the three models aforementioned are listed in Table I, and the plot of t/q_t vs. t based on linear form of the pseudo-second-order kinetic model is shown in the inset of Figure 8(a). It can be clearly seen that the correlation coefficient

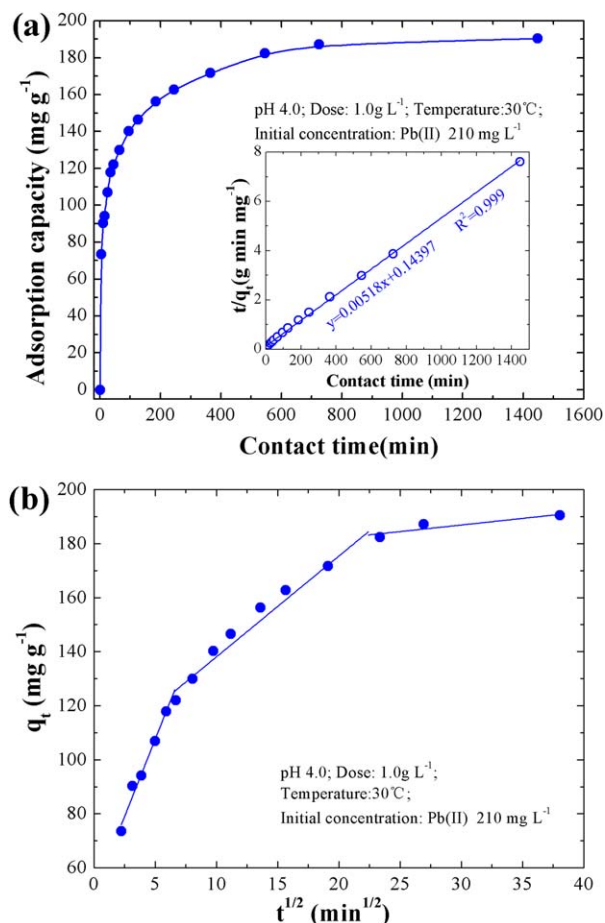


Figure 8. (a) Effect of contact time on adsorption of Pb(II) ions by EDTA/chitosan/PMMS (inset: The pseudo-second-order kinetic model plot for the adsorption of Pb(II) ions on the adsorbent); (b) intraparticle diffusion kinetic model fits for the adsorption of Pb(II) ions on EDTA/chitosan/PMMS. [Color figure can be viewed in the online issue, which is available at wileyonlinelibrary.com.]

Table I. Pseudo–First-Order, Pseudo–Second-Order, and Intraparticle Diffusion Kinetic Model Parameters Obtained from the Sorption of Pb(II) on EDTA/Chitosan/PMMS at pH 4 and 30°C

| C_0 (mg L ⁻¹) | $q_{e,exp}$ (mg g ⁻¹) | Pseudo–first-order model | | | Pseudo–second-order model | | | Intraparticle diffusion model (mg g ⁻¹ min ^{-1/2}) | | |
|--------------------------------|--------------------------------------|--------------------------------------|---|-------|--------------------------------------|--|-------|---|-----------|-----------|
| | | $q_{e,cal}$ (mg g ⁻¹) | $k_1 \times 10^3$ (min ⁻¹) | R^2 | $q_{e,cal}$ (mg g ⁻¹) | $k_2 \times 10^4$ (g mg ⁻¹ min ⁻¹) | R^2 | $k_{i,1}$ | $k_{i,2}$ | $k_{i,3}$ |
| 210.2 | 190.4 | 76.88 | 3.41 | 0.944 | 192.9 | 1.867 | 0.999 | 11.44 | 3.73 | 0.49 |

(R^2) value of the pseudo–second-order model is much higher than that of the pseudo–first-order model, and the theoretical calculated $q_{e,cal}$ values predicted from the pseudo–second-order model are much more close to the experimental ones ($q_{e,exp}$) than that from the pseudo–first-order model. The results indicate that the adsorption mechanism described by the pseudo–second-order model is more reasonable than that of the pseudo–first-order model, and chemical adsorption might be the rate determining step for the adsorption of Pb(II) ions on EDTA/chitosan/PMMS.¹⁷

The plot of the intraparticle diffusion model for Pb(II) ions adsorption on EDTA/chitosan/PMMS is given in Figure 8(b). It may be seen that there are three separate linear portions appeared in the plot. The first straight portion is attributed to the film diffusion¹⁷ or boundary layer diffusion effect,²⁹ and the second or third slopes might be due to intraparticle diffusion effect.^{17,29} Moreover, the diffusion rate constants in the three portions follow the order of $k_{id,1} > k_{id,2} > k_{id,3}$, which are presented in Table I. These results indicate that the film diffusion plays very important role in the initial stage of adsorption, which suggests that fast boundary layer diffusion of Pb(II) ions in the solutions was taken place. Thereafter, the diffusion rates became very slow for Pb(II) to migrate into the pores of the adsorbents, which were the least accessible sites of adsorption.

However, as presented in Figure 7(b), the intraparticle diffusion plots do not pass through the origin, and multilinear portions are observed, indicating that intraparticle diffusion is not the only rate-limiting step in the adsorption. This is further confirmed by intraparticle diffusion coefficient (D , cm² s⁻¹), which could be calculated from the following equation:^{29,30}

$$D = \frac{0.03r^2}{t_{1/2}} \quad (5)$$

where r (cm) is the average radius of the sorbent particle and $t_{1/2}$ (min) is the time for half of the sorption.

According to the Michelson *et al.*,^{29,30} a D value of the order of 10⁻¹¹ cm² s⁻¹ is indicative of intraparticle diffusion as rate determining step. In this work, the mean particle diameter (d_p) of EDTA/chitosan/PMMS was determined to be 57.5 μm by laser particle analyzer, the time for half of the sorption was 225 min [calculated from the second linear portion shown in Figure 8(b)], therefore, D value for this investigation is calculated to be 1.102 × 10⁻⁹ cm² s⁻¹, which is more than 2 order of magnitude higher compared with 10⁻¹¹ cm² s⁻¹. This result indicates that the intraparticle diffusion is not the only rate controlling step, other mechanism such as boundary layer diffusion is also involved.²⁹

Adsorption Isothermal Study

The adsorption isotherm of Pb(II) ions adsorbed on EDTA/chitosan/PMMS is presented in Figure 9, and the experimental data were further fitted by three common adsorption isotherm models: Langmuir, Freundlich, and Dubinin–Radushkevich (D–R). The Langmuir isotherm model³¹ predicts that a monolayer adsorption happens on a homogeneous surface, and its linear form equation can be expressed as follows:

$$\frac{C_e}{q_e} = \frac{1}{q_m K_L} + \frac{C_e}{q_m} \quad (6)$$

where q_e is the uptake capacity of Pb(II) at equilibrium concentration (mg g⁻¹), and q_m is the maximum adsorption capacity of adsorbent (mg g⁻¹); C_e represent the equilibrium concentration of Pb(II) ions in solution; K_L is the Langmuir binding constant which is related to the energy of adsorption (L mg⁻¹).

The Freundlich isotherm model³² is based on the assumption of the adsorption on the heterogeneous surfaces, and the amount of solute adsorbed on adsorbent increase infinitely with the concentration rise. The model can be represented by the following equation:

$$\ln q_e = \frac{1}{n} \ln C_e + \ln K_F \quad (7)$$

where K_F is Freundlich constant (L mg⁻¹) related to adsorption capacity, and n is the heterogeneity factor related to adsorption intensity.

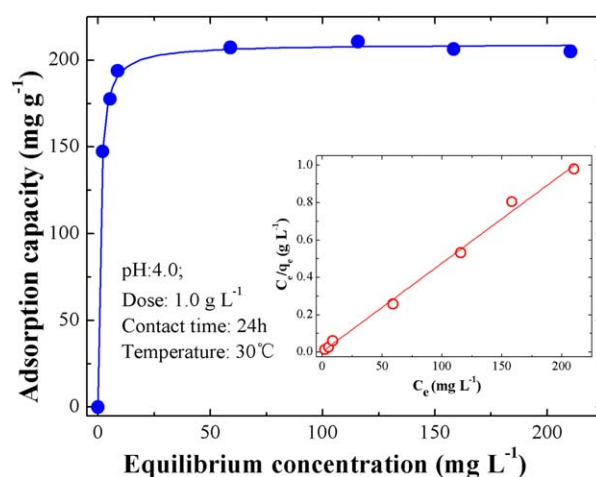


Figure 9. Adsorption isotherm for Pb(II) ions on EDTA/chitosan/PMMS (inset: Langmuir isotherm plot for adsorption of Pb(II) on EDTA/chitosan/PMMS). [Color figure can be viewed in the online issue, which is available at wileyonlinelibrary.com.]

Table II. Parameters Obtained from the Langmuir, Freundlich, and Dubinin–Radushkevich Isothermal Models for Adsorption of Pb(II) on EDTA/Chitosan/PMMS at pH 4 and 30°C

| T (°C) | $q_{m,exp}$ (mg g ⁻¹) | Langmuir | | | Freundlich | | | Dubinin–Radushkevich model | | |
|--------|--------------------------------------|--------------------------------|--------------------------------------|-------|------------|-------|-------|--------------------------------------|---|-------|
| | | K_L (L mg ⁻¹) | $q_{m,cal}$ (mg g ⁻¹) | R^2 | K_F | n | R^2 | $q_{m,cal}$ (mg g ⁻¹) | $K_D \times 10^3$ (mol ² kJ ⁻²) | R^2 |
| 30 | 210.6 | 1.4098 | 210.8 | 0.999 | 220.8 | 16.04 | 0.716 | 217.4 | 2.57 | 0.902 |

Dubinin–Radushkevich (D–R) model^{33–35} is generally used to predict whether the adsorption process is physical adsorption or chemical adsorption. The D–R equation is expressed as follows:

$$\ln q_e = \ln q_m - K_D \varepsilon^2 \quad (8)$$

where K_D is the constant related to the mean free energy of sorption (mol² kJ⁻²), q_m is the theoretical saturation capacity (mg g⁻¹) of the D–R model, and ε is the Polanyi potential. The values of ε can be calculated from the following equation:

$$\varepsilon = RT \ln \left(1 + \frac{1}{C} \right) \quad (9)$$

The adsorption isotherm parameters simulated from the three isothermal models mentioned above are listed in Table II, and the plot of C_e/q_e versus C_e based on the linear form of the Langmuir model are given in the inset of Figure 9. According to the inset of Figure 9 and Table II, the Langmuir model fits better with the experimental data of isothermal study due to the highest correlation coefficients (0.999), which indicates a monolayer adsorption of Pb(II) ions on EDTA/chitosan/PMMS. Moreover, the maximum uptake capacity (q_m) for Pb(II) ions on the adsorbent estimated from the Langmuir equation is 210.8 mg g⁻¹, which is very consistent with that of experimental ones ($q_{e,exp}$).

On the other hand, from the D–R isothermal model, the mean free energy of the adsorption (E) related to the D–R constant K_D provides information about chemical or physical adsorption,^{33–35} which is expressed in the following equation:

$$E = \frac{1}{(2K_D)^{1/2}} \quad (10)$$

If the value of E is between 8 and 16 kJ mol⁻¹, the adsorption process could be predicted as a chemical adsorption, but if it is lower than 8 kJ mol⁻¹, physical adsorption process is followed.^{34,35} The E value for the adsorption of Pb²⁺ on EDTA/chitosan/PMMS was calculated to be 13.96 kJ mol⁻¹ from the K_D value in Table II, which indicates the adsorption processes were chemisorptions. This is in agreement with the results aforementioned in the kinetic studies, and further confirms that strong chelating effects existed between Pb²⁺ and EDTA/chitosan/PMMS.

The comparison of the maximum adsorption capacities of Pb(II) onto different chitosan derivatives are summarized in Table III. It can be seen that the maximum uptake capacity (q_m , mg g⁻¹) of EDTA/chitosan/PMMS for Pb(II) is much higher than that of most of the adsorbents in Table III, however, it is lower than that of chitosan-EDTA complex, which was simply synthesized by reacting chitosan with EDTA anhydride.⁴⁰ It is notable that EDTA-modified chitosan grafted on EDTA/chitosan/PMMS was mainly responsible for adsorption of Pb(II) ions, and the organic polymer grafted ratio on the adsorbent was about 64.4% according to TGA analysis results. Therefore, the maximum adsorption capacity based on the weight of EDTA-modified chitosan on the adsorbent is estimated to be 327.6 mg g⁻¹, which is slightly higher than that of chitosan-EDTA complex (310.8 mg g⁻¹). Moreover, EDTA/chitosan/PMMS also showed excellent magnetic separability.

Table III. Comparison of the Maximum Adsorption Capacities of Chitosan Derivatives

| Adsorbent | Adsorption capacity (mg g ⁻¹) | Condition | References |
|-----------------------------------|---|--------------|------------|
| Chitosan modified by benzaldehyde | 3.2906 | 25°C, pH 4 | 36 |
| Chitosan/magnetite | 63.3 | 25°C, pH 6 | 37 |
| EDTA-Chi : TEOS 2 : 15 | 126.4 | 22°C, pH 3 | 17 |
| EDTA-Chi : TEOS 2 : 30 | 89.1 | 22°C, pH 3 | 17 |
| CMS | 9.32 | 25°C, pH 5 | 19 |
| EDCMS | 123 | 25°C, pH 5 | 19 |
| m-Chitosan/PVA/CCNFs | 171 | 25°C, pH 4.5 | 38 |
| Triethylene-tetramine grafted | | | |
| Magnetic chitosan | 370.63 | 25°C, pH 6.0 | 39 |
| Chitosan-EDTA complex | 310.8 | | 40 |
| EDTA/chitosan/PMMS | 211 | 30°C, pH 4 | This work |

Although the maximum adsorption capacity of triethylene-tetramine grafted magnetic chitosan (370.63 mg g^{-1} at pH 6) is much higher than that of EDTA/chitosan/PMMS. Its adsorption capacity for Pb(II) ions would decrease to half of its maximum value at pH 4 due to protonation of triethylene-tetramine.³⁹ Similarly, the uptake capacity of m-chitosan/PVA/CCNFs would decrease to a quarter of its maximum value when solution pH was 2. Nevertheless, the adsorption capacities of EDTA/chitosan/PMMS for Pb(II) ions would be kept almost unchanged in the pH range of 2 to 6, because EDTA groups have excellent tolerance to low pH value according to the results of pH effects mentioned above.

Effect of Temperature and Thermodynamics Study

It is well known that temperature plays an important role in adsorption. The results of the effect of adsorption temperature (ranged from 298 to 318 K) are shown in Table IV, and the thermodynamic parameters were predicted by using the following equations:^{41–43}

$$K_c = \frac{C_A}{C_e} \quad (11)$$

$$\Delta G^\circ = -RT \ln K_c \quad (12)$$

$$\ln K_c = -\frac{\Delta H^\circ}{RT} + \frac{\Delta S^\circ}{R} \quad (13)$$

where C_A is the concentration of Pb(II) adsorbed on the adsorbent, while C_e represent the equilibrium concentration of Pb(II) ions. K_c is the thermodynamic equilibrium constant.⁴¹ R is the gas constant ($8.314 \text{ J mol}^{-1} \text{ K}^{-1}$), and T is the absolute temperature (K). ΔG° , ΔH° , and ΔS° are the standard Gibbs free energy, enthalpy and entropy changes, respectively.

ΔH° and ΔS° were obtained from the slope and the intercept of the plot of $\ln K_c$ versus $1/T$ based on the van't Hoff equation [eq. (13)], which is depicted in Table IV. The negative value of ΔH° reveals an exothermic nature of the adsorption, and the negative value of ΔS° suggests the decreasing randomness at the adsorbent/adsorbate interface during the adsorption processes.⁴⁴ Moreover, the negative values of ΔG° presented in Table IV indicates that all the adsorption processes are spontaneous, and the value increase with the increasing of temperature, which means a greater driving force for adsorption at low temperatures.⁴⁵

Desorption and Reusability Studies

From practical point of view, reusability is an important feature of an advanced adsorbent. Although the adsorption capacities

Table IV. Thermodynamic Parameters for the Adsorption of Pb(II) Ions onto EDTA/Chitosan/PMMS

| T (K) | K_c | Thermodynamic parameters | | | R^2 |
|-------|-------|---|---|--|-------|
| | | ΔG° (kJ mol ⁻¹) | ΔH° (kJ mol ⁻¹) | ΔS° (J mol ⁻¹ K ⁻¹) | |
| 298 | 9.183 | -5.50 | -33.09 | -92.98 | 0.955 |
| 308 | 5.095 | -4.17 | | | |
| 318 | 3.981 | -3.65 | | | |

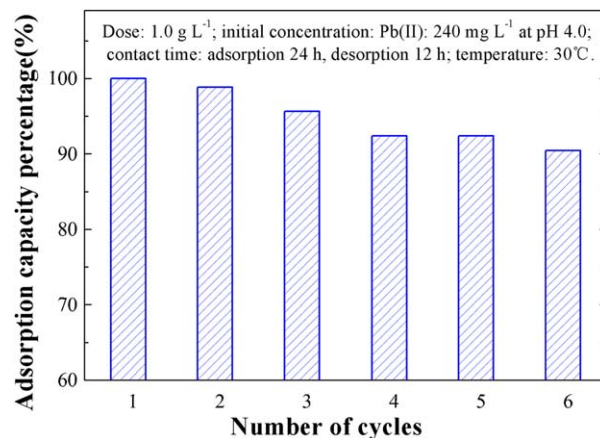


Figure 10. Reusability of EDTA/chitosan/PMMS for removal of Pb(II) ions. [Color figure can be viewed in the online issue, which is available at wileyonlinelibrary.com.]

of EDTA/chitosan/PMMS are very high in the acid conditions, erosion of magnetic cores might be taken place in the strong acid solution. Therefore, 0.1M of Na₂EDTA solution instead of acid was selected as eluent for regeneration of the adsorbents. The relative percentage changes of the adsorption capacities of Pb(II) on EDTA/chitosan/PMMS during 5 times reuse are illustrated in Figure 10. It is observed that the adsorption capacity of the recycled adsorbent still retains above 90% of capacity of the fresh adsorbent after the fifth adsorption-desorption cycle, which indicates that EDTA/chitosan/PMMS can be used repeatedly as efficient adsorbents for practical wastewater treatment.

CONCLUSION

A novel magnetic adsorbent of EDTA/chitosan/PMMS was simply synthesized by reacting chitosan with EDTA anhydride in presence of PEI-coated magnetic microspheres. The characterization results of the adsorbents by FESEM, FT-IR, and TGA confirmed that EDTA modified chitosan was successfully grafted on the magnetic cores. The magnetic adsorbents of EDTA/chitosan/PMMS showed excellent adsorption properties for removal of Pb(II) ions from aqueous solution due to its high uptake capacities at low pH values. Moreover, good magnetic separability and reusability of the adsorbent will make it become a promising candidate for heavy metal pollution cleanup in the practical wastewater treatment.

ACKNOWLEDGMENTS

The authors thank the financial support provided by Ministry of Water Resource, Public Interest Scientific Research Fund (No. 201501019).

REFERENCES

- Oncel, M. S.; Muhcu, A.; Demirbas, E.; Kobya, M. J. *Environ. Chem. Eng.* **2013**, *1*, 989.
- Naeem, A.; Saddique, M. T.; Mustafa, S.; Kim, Y.; Dilara, B. *J. Hazard. Mater.* **2009**, *168*, 364.
- Bessbousse, H.; Rhilalou, T.; Verch'ere, J. F.; Lebrun, L. J. *Membr. Sci.* **2008**, *307*, 249.

4. Beauchesne, I.; Meunier, N.; Drogui, P.; Hausler, R.; Mercier, G.; Blais, J. F. *J. Hazard. Mater.* **2005**, *120*, 201.
5. Cui, Y.; Ge, Q. C.; Liu, X. Y.; Chung, T. S. *J. Membr. Sci.* **2014**, *467*, 188.
6. Ghasemi, M.; Naushad, M.; Ghasemi, N.; Khosravi-Fard, Y. *J. Ind. Eng. Chem.* **2014**, *20*, 2193.
7. Akar, T.; Sibel Tunali, S. *Bioresour. Technol.* **2006**, *97*, 1780.
8. Liu, B. J.; Lv, X.; Meng, X. H.; Yu, G. L.; Wang, D. F. *Chem. Eng. J.* **2013**, *220*, 412.
9. Varma, A. J.; Deshpande, S. V.; Kennedy, J. F. *Carbohydr. Polym.* **2004**, *55*, 77.
10. Wan Ngah, W. S.; Teong, L. C.; Hanafiah, M. A. K. M. *Carbohydr. Polym.* **2011**, *83*, 1446.
11. Nguyen, T. A. H.; Ngo, H. H.; Guo, W. S.; Zhang, J.; Liang, S.; Yue, Q. Y.; Li, Q.; Nguyen, T. V. *Bioresour. Technol.* **2013**, *148*, 574.
12. Wang, J. L.; Chen, C. *Bioresour. Technol.* **2014**, *160*, 129.
13. Radwan, A. A.; Alanazi, F. K.; Alsarra, I. A. *Molecules* **2010**, *15*, 6257.
14. Wu, S. J.; Liou, T. H.; Yeh, C. H.; Mi, F. L.; Lin, T. K. *J. Appl. Polym. Sci.* **2013**, *127*, 4573.
15. Muzzarelli, R. A. A.; Tanfani, F. *Pure Appl. Chem.* **1982**, *54*, 2141.
16. Repo, E.; Warchol, J. K.; Kurniawan, T. G.; Sillanpää, M. *Chem. Eng. J.* **2010**, *161*, 73.
17. Repo, E.; Warchol, J. K.; Kurniawan, B. A.; Sillanpää, M. *J. Colloid Inter. Sci.* **2011**, *358*, 261.
18. Qin, R. H.; Li, F. S.; Chen, M. Y.; Jiang, W. *Appl. Surf. Sci.* **2009**, *256*, 27.
19. Ren, Y.; Abbood, H. A.; He, F. B.; Peng, H.; Huang, K. X. *Chem. Eng. J.* **2013**, *226*, 300.
20. Deng, H.; Li, X.; Peng, Q.; Wang, X.; Chen, J.; Li, Y. *Angew. Chem. Int. Ed.* **2005**, *44*, 2782.
21. Zhang, F. W.; Zhu, Z. Z.; Dong, Z. P.; Cui, Z. K.; Wang, H. B.; Hu, W. Q.; Zhao, P.; Pan Wang, Wei, S. Y.; Li, R.; Ma, J. T. *Microchem. J.* **2011**, *98*, 328.
22. Monier, M.; Ayad, D. M.; Wei, Y.; Sarhan, A. A. *React. Funct. Polym.* **2010**, *70*, 257.
23. Gwen, L.; Imelda, K.; Barry, D.; Adrienne, C. -T.; Llewellyn, R.; Peter, F.; Lisbeth, G. *Biomacromolecules* **2007**, *8*, 2533.
24. Maliyekkal, S. M.; Shukla, S.; Philip, L.; Nambi, I. M. *Chem. Eng. J.* **2008**, *140*, 183.
25. Ge, F.; Li, M. M.; Ye, H.; Zhao, B. X. *J. Hazard. Mater.* **2012**, *211*, 366.
26. Lagergren, S.; Kung, S. V. *Hand* **1898**, *24*, 1.
27. Ho, Y. S.; McKay, G. *Chem. Eng. J.* **1998**, *70*, 115.
28. Weber, W.; Morris, J.; Sanit, J. *Eng. Div. Am. Soc. Civ. Eng.* **1963**, 8931.
29. Hasan, S. H.; Singh, K. K.; Prakash, O.; Talat, M.; Ho, Y. S. *J. Hazard. Mater.* **2008**, *152*, 356.
30. Michelson, L. D.; Gideon, P. G.; Pace, E. G.; Kutsal, L. In Bulletin 74, Removal of Soluble Mercury from Waste Water By Complexing Techniques, Virginia: US Department Industry, Office of the Water Research and Technology, **1975**, p 74.
31. Langmuir, I. *J. Am. Chem. Soc.* **1916**, *38*, 2221.
32. Freundlich, H. Z. *Phys. Chem.* **1906**, *57*, 385.
33. Laus, R.; Costa, T. G.; Szpoganicz, B.; Fávere, V. T. *J. Hazard. Mater.* **2010**, *183*, 233.
34. Chen, A. H.; Chen, S. M. *J. Hazard. Mater.* **2009**, *172*, 1111.
35. Tunali, S.; Akar, T.; Özcan, A. S.; Kiran, I.; Özean, A. *Sep. Purif. Technol.* **2006**, *47*, 105.
36. Duan, L. H.; Guo, S. Y.; Yang, J. Q. *Adv. Chem. Eng. Sci.* **2011**, *2*, 101.
37. Tran, H. V.; Tran, L. D.; Nguyen, T. N. *Mater. Sci. Eng. C* **2010**, *30*, 304.
38. Zhou, Y. M.; Fu, S. Y.; Zhang, L. L.; Zhan, H. Y.; Levit, M. V. *Carbohydr. Polym.* **2014**, *101*, 75.
39. Kuang, S. P.; Wang, Z. Z.; Liu, J.; Wu, Z. C. *J. Hazard. Mater.* **2013**, *260*, 210.
40. Inoue, K.; Ohto, K.; Yoshizuka, K.; Yamaguchi, T.; Tanaka, T. *Bull. Chem. Soc. Jpn.* **1997**, *70*, 2443.
41. Lian, L.; Guo, L.; Guo, C. *J. Hazard. Mater.* **2009**, *161*, 126.
42. Rao, R. A. K.; Kashifuddin, M. *Adsorpt. Sci. Technol.* **2012**, *30*, 127.
43. Ayanda, O. S.; Fatoki, O. S.; Adekola, F. A.; Ximba, B. J. *Mar. Pollut. Bull.* **2013**, *72*, 222.
44. Gupta, V.; Mittal, A.; Gajbe, V.; Mittal, J. *Ind. Eng. Chem. Res.* **2006**, *45*, 1446.
45. Chen, Y. F.; He, F. B.; Ren, Y.; Peng, H.; Kaixun Huang, K. X. *Chem. Eng. J.* **2014**, *249*, 79.